TABLE IV. Transition matrix elements in (Ry) for selected transitions.

Transition[a]	$L_2' \rightarrow L_1$	$L_1^d \rightarrow L_2'$	$L_3^1 \rightarrow L_2'$	$X_5 \rightarrow X_4'$
$\frac{2}{3}P_{ij}^2/m$	3.17	0.533	0.015	0.250

[a] The matrix elements are calculated using the eigenvalues given in Ref. 14 [F. M. Mueller (private communication)].

11). From the experimental ϵ_2 we estimate a total contribution of about 30%, extrapolating the contribution of the background below 4.1 eV to about 4.65 eV. The high percentage of $L_2' \rightarrow L_1$ transitions as calculated from theory is consistent with the pronounced edge in the experimental ϵ_2 and with the large W_{44} as well. This leads again to the conclusion that the observed structure in ϵ^2 and $\Delta\epsilon_2$ at 4.3 eV is caused by the FS $\rightarrow L_1$ transition.

Another striking feature of the functions W_{ij} is the vastly different magnitude of W_{44} and $W_{11}-W_{12}$. The maximum $\Delta\epsilon_2$ observed for trigonal shear strain is nine times the corresponding value for tetragonal shear strain (the amount of the strain being the same). This is partly due to the different degree of localization in k space discussed above and partly to the difference in the oscillator strength (Table IV). The small oscillator strength for $X_5 \rightarrow X_4'$ as compared with the one for $L_2' \rightarrow L_1$ suggests that there is no pronounced structure in ϵ_2 around 4.0 eV, and indeed the experimental curve is nearly flat in this region. However, we believe to have resolved a tiny hump in our room-temperature measurements of ϵ_2, as shown in Fig. 12. The reflectance at liquid He temperatures[30] shows a well-resolved structure at about the same energy. The transition does show up clearly as a minimum in $W_{11}-W_{12}$ at room temperature.

The hydrostatic change ($W_{11}+2W_{12}$) and the change with trigonal shear strain (W_{44}) have the same shape between 4 and 4.5 eV. The position of the maximum is 4.3 eV in both cases. This suggests that both effects are due to the FS $\rightarrow L_1$ transition. The two functions differ between 4.5 and 5 eV, where $W_{11}+2W_{12}$ exhibits an additional shoulder around 4.8 eV, whereas W_{44} approaches zero rapidly. This behavior can be explained assuming transitions from the bottom of the d bands to the FS. As in the case of the 2.1-eV edge (where the top of the d bands provides the initial states), these transitions originate from general points of the BZ. This explains the lack of response to shear strain. The transitions will of course change under hydrostatic strain. The situation is equivalent to the one at the 2.1-eV edge, where only hydrostatic strain produces a significant change in ϵ_2.

Experimental Deformation Potentials

The assignment of the structure observed in W_{ij} and ϵ_2 has been established in the preceding sections. This information can be used to calculate the deformation potentials of the corresponding transitions from the experiments, i.e., the difference in the deformation potentials of the final and the initial state. Additional knowledge is required to do so, namely, the slope $d\epsilon_2/d(\hbar\omega)$ of that part of ϵ_2 which is responsible for the observed structure in W_{ij} and the selection rules (required for the shear-strain coefficients only). Furthermore, it must be possible to separate that part of W_{ij} which is due to a change of the energy levels from the ones due to modifications of the transition matrix elements M and of the density of states J.

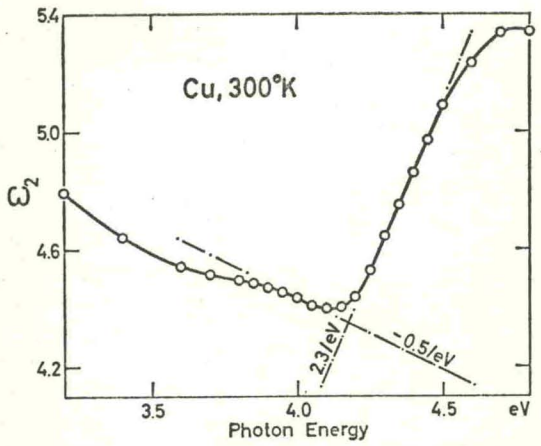

FIG. 12. A blow-up of the imaginary part of the dielectric constant of Cu at room temperature around 4 eV, showing weak structure slightly below 4 eV. The slope of the edge at 4.3 eV and the slope of the background which were used to calculate the deformation potentials of the $E_F \rightarrow L_1$ transition are also included.

The slope of the edge at 2.1 eV is large; modifications due to a background of transitions other than $L_3^u \rightarrow$ FS (e.g., free carrier absorption) will be small. The selection rules are not needed because only hydrostatic strain produces a pronounced change in ϵ_2. The changes in M and J produced by a hydrostatic strain will be much smaller than the ones produced by shear strain, in which case they are required by symmetry.[7] Only $W_{11}+2W_{12}$ is large at this edge, which shows that changes of M and J contribute very little to $W_{11}+2W_{12}$. The deformation potential will be given quite accurately by the maximum value of $W_{11}+2W_{12}$ and by the uncorrected slope of ϵ_2.

As discussed above, the 2.1-eV edge is due to nonlocalized transitions; the transitions with lowest energy have k vectors terminating just outside the neck, but at slightly higher energies transitions with k vectors located in other parts of the BZ will contribute. The deformation potential determined from the energy shift of the edge will be an average over the deformation potentials of all transitions which contribute. However, the top of the d bands is rather flat, particularly the portion $L_3^u - Q_+$, and it will remain flat if the volume of the crystal is changed. Thus the deformation potentials of transitions contributing to the edge differ only slightly from each other. We therefore no

[30] M. A. Biondi and J. A. Rayne, Phys. Rev. 115, 1522 (1959).